Renewable Energy 83 (2015) 615–625

Contents lists available at ScienceDirect

Renewable Energy

journal homepage: www.elsevier.com/locate/renene

Impact of the throat sizing on the operating parameters in an experimental fixed bed gasifier: Analysis, evaluation and testing

Lina Montuori [a,*], Carlos Vargas-Salgado [b], Manuel Alcázar-Ortega [b]

[a] State University of New York at Buffalo, Department of Electrical Engineering, 230 Davis Hall, 14260 Buffalo, NY, USA
[b] Universidad Politécnica de Valencia, Institute for Energy Engineering, Camino de Vera, s/n, edificio 8E, escalera F, 5ª planta, 46022 Valencia, Spain

A R T I C L E I N F O

Article history:
Received 18 October 2014
Accepted 28 April 2015
Available online xxx

Keywords:
Throat size
Downdraft gasifier
Pressure drop
Biomass
Syngas
Renewable resources

A B S T R A C T

The aim of this research is to contribute into the diffusion of biomass power systems by analyzing and testing the throat sizing influence on the operation of a gasification plant coupled with an internal combustion engine. In order to do this, the assessment of the proper operation range for some of the driving process parameters has been carried out. The analysis has been focused on such parameters as pressure drop of the fixed bed reactor, the inlet air flow, the syngas production, electrical power production and efficiency, looking for improving the performance and guaranteeing the proper system operation. Two different campaigns of tests have been carried out for figuring out the best design on the reactor. Based on this analysis, the most convenient throat diameter has been determined (in this case, around 10 cm), producing an increment in the production of syngas of about 31%. This modification has demonstrated also an increment of the electrical power produced by the gasification plant of about 40%, which means an increment in the motor generator efficiency of 35%.

1. Introduction

Continuous efforts have been made in exploration of renewable energy resources for a sustainable development as a consequence of the global economic crisis that has affected the energy market and the global economy during the recent years [1]. Among all of the renewable resources, biomass is the only one which contains carbon source to be converted into solid, liquid and gaseous products, and further into electricity, heat and transport fuels. Currently, biomass is the fourth largest energy source in the world after coal, petroleum and natural gas [2,3].

Like wind, solar, and other renewable energy sources, biomass can make a positive impact on the atmosphere facing the climate change induced by the green gas emissions (GHG) and decreasing the dependence on fossil fuels that still account for 80% of primary energy consumption [4]. The energy obtained from biomass, based on short rotation forestry and other energy crops, can significantly contribute towards the renewable energy target of the European Union, EU 20% by 2020 [5]. Biomass fuels and residues can be turned into energy via different processes (e.g. physical, thermal, chemical, and biological conversion) and all biomass can be burned in thermo-chemical conversion plants (i.e. combustion to produce steam useful for power production) [6]. Among the thermo-chemical processes, a considerable interest into biomass gasification has been growing worldwide in the last decades [7,8]. As a matter of fact, since any biomass material can undergo gasification, the gasification process is much more attractive than others such as ethanol production or biogas, where only selected biomass materials can produce the fuel [9]. The United States Department of Energy (DOE) has had a major goal in the development of cost competitive gasification technologies for the power production from renewable biomass crops [10,11]. Furthermore, an extensive review in Europe and Canada identified 50 manufacturers offering ‘commercial’ gasification plants from which 75% of the designs were downdraft type [12]. The downdraft technology owns the favorable characteristics of flexible adaptation of the syngas production to the load; low sensitivity to charcoal dust and tar content of the fuel (0.015–3 g/Nm^3); shorter time of ignition (5–20 min) and to reach the operating temperature than an updraft gasifier (30–60 min) [7]. Depending on the fuel used (its final form, size and moisture content) these technical aspects make downdraft technology preferable to others [13]. The gasification converts

* Corresponding author. Tel.: +1 716 418930.
E-mail addresses: linamont@buffalo.edu (L. Montuori), carvasa@upvnet.upv.es (C. Vargas-Salgado), malcazar@iie.upv.es (M. Alcázar-Ortega).

http://dx.doi.org/10.1016/j.renene.2015.04.068
0960-1481/

Nomenclature

$\dot{m}_a$	air mass flow (kg/s)
$\dot{m}_g$	syngas mass flow (kg/s)
g	gravitational acceleration (m/s^2)
ρ_a	air density (kg/m^3)
ρ_g	syngas density (kg/m^3)
ϕ_1	first campaign throat diameter (m)
ϕ_2	second campaign throat diameter (m)
A/S	air–syngas rate
A_0	inlet air section (m^2)
A_1	throat section at diameter ϕ_1 (m^2)
A_2	throat section at diameter ϕ_2 (m^2)
v_0	air inlet speed (m/s)
v_1	outlet gas speed at the section A_1 (m/s)
v_2	outlet gas speed at the section A_2 (m/s)
$\Delta z_2 = z_0 - z_2$	elevation betweens the measuring points (m)
$\dot{Q}_a$	inlet air volumetric flow (m^3/s)
P_0	atmospheric pressure (bar)
P_1	syngas pressure at the throat section A_1 (bar)
P_2	syngas pressure at the throat section A_2 (bar)
P_{elec}	electrical power at the generator terminals (kW)
$\Delta P_1 = P_0 - P_1$	bed pressure drop with ϕ_1 throat diameter (bar)
$\Delta P_2 = P_0 - P_2$	bed pressure with ϕ_2 throat diameter (bar)
L	length of the reduction zone (m)
d	equivalent diameter of the biomass particle (m)
u	superficial velocity (m/s)
Y	fluid viscosity (Pa·s)
ϵ	porosity
ρ_m	density of the suspension (kg/m^3)

biomass into a combustible gas mixture called syngas (synthesis gas) by its partial oxidation at high temperatures, typically in the range 800–1000 °C [8]. The syngas constitutes a mixture of carbon monoxide (CO), hydrogen (H_2), methane (CH_4), small quantities of other light hydrocarbons (C_nH_m), carbon dioxide (CO_2) and steam (H_2O), besides the nitrogen (N_2) present in the air supplied for the reaction [14].

It is a vital building block for the petrochemical industry and it is an important intermediate for synthesis of large numbers of industrial products. Thus, maximizing the syngas yield from biomass will largely promote the biomass utilization with high efficiency [15]. The syngas can be used to run internal combustion engines both compression and spark ignition, as substitute for furnace oil in direct heat applications or to produce, in an economically viable way, methanol which is useful both as fuel for heat engines as well as chemical feedstock for industries [16].

The gasification plant on which the experimental analysis is focused, adopts a downdraft fixed bed technology in which the air passes from the tuyeres in the downdraft direction. The gasifier has been coupled with an internal combustion engine (ICE) for a power production of 5 kWe. The ICE, traditionally working with gasoline, has been adapted to work with syngas characterized by a lower heating value (LHV) generally between 4 and 6 MJ/m^3 [17]. The gasifier is fueled with pellets, based on lignocellulosic biomass belonged to woody energy crops.

Although regional and national policies in different countries attempt to dampen their use and increase alternative energy, recent studies on biomass gasification for small scale application have demonstrated that it could be currently considered a quite mature technology [18–21]. Notwithstanding that greater efforts are still required in research to achieve further advances in the diffusion of gasification technologies [14,22,23].

In literature, different studies can be found on fixed bed gasification process. Previous works have studied the performance of the biomass gasifier system in terms of producer gas composition, gas production rate, zone temperatures and cold gas efficiency [24–26]. Guangui et al. show as preheating the gasifying air improves the outputs of the gasification process since the air flow rate has a significant effect on the quality of the producer gas [27]. The influence of the heating value and equivalent ratio on the performance of a downdraft fixed bed gasifier using different throat diameters was also presented by Gunarathne et al. [28]. However, they did not assess the relationship between throat diameter and bed pressure drop. The original mark of the present work lies in the analysis of the design of the throat on the gasification parameters, inlet air flow and bed pressure drop. Based on this analysis, the most convenient throat diameter has been determined, resulting in an increment in the production of syngas, efficiency and power generation. A methodology to evaluate and assess the behavior of the bed pressure drop and air inlet flow in function of the throat diameter has been implemented in order to achieve the feasible management of a downdraft fixed bed gasifier. The application of this methodology would allow designers and energy managers to increase the syngas production and, consequently, the power generation. Therefore, a higher reliability of the gasification plant can be achieved. Finally, the relationships between the characteristic process parameters have been investigated in order to favorite the widespread of this technology and enabling the gasification plant to properly operate at full capacity.

The paper is organized as follows: an overview about the experimental setup of the downdraft fixed bed gasification technology adopted in this study is presented in Section 2. Section 3 presents the proposed methodology for the evaluation and assessment of the effect of the gasifier throat diameter on the driving process parameters. In Section 4, the description of the modification performed on the gasification plant and some considerations about the gasification process parameters taken into account in the study are explained. The methodology is applied to a gasification plant designed at the Institute for Energy Engineering of Valencia (IIE), Spain, in Section 5. Finally, some conclusions are stated in Section 6.

2. Experimental setup of the gasification plant

The influence of the throat sizing on the characteristic process parameters was investigated and then tests were carried out on the experimental gasification plant developed by the Laboratory of Distributed Energy Resources (LabDER) of the IIE [18]. The initial design of the reactor throat was modified so that the diameter of the throat was increased with a constant geometry.

2.1. Characterization of the lignocellulosic biomass: pellets

During the tests, the power plant was fueled with waste biomass derived from different woody energy crops. Cellulose, hemicellulose and lignin and extractives are found to be the major components of the woody biomass. The biomass composition in terms of these elements is reported in Table 1, including the proximate and ultimate analysis. Proximate analysis gives the composition of the biomass in terms of gross components: moisture (M), volatile

Table 1
Pellets characterization.

Chemical analysis							
Ultimate analysis	**C**	**H**	**O**	**N**	**S**	**H/C**	**O/C**
	47%	7%	45%	2%	0%	15%	96%
Proximate analysis	**FC**	**VM**	**ASH**	**M**	**HHV (kCal/kg)**	**LHV (kCal/kg)**	**LHV/HHV**
	15%	76%	2%	6%	4.282	3.880	91%
Component analysis							
Cellulose (wt.%, dry)		**Lignin (wt.%, dry)**		**Hemicellulose (wt.%, dry)**		**Extractives (wt.%, dry)**	
54.6		16.2		27		2.2	

matter (VM), ash (ASH), and fixed carbon (FC). Ultimate analysis quantifies carbon, hydrogen, and oxygen fractions and it is reported using the $C_xH_yO_z$ formula where x, y, and z represents the elemental fractions of C, H, and O, respectively. Biomass size is a factor that needs to be considered in gasification processes. Through a pelleting process the waste biomass has been prepared into pellets with a diameter between 4 and 6 mm and a length from 10 to 12 mm. Previous studies conducted on a downdraft reactor have demonstrated that an increase in particle diameter (d) above 6 mm led to lower biomass consumption rates, fuel/air equivalent ratios, maximum process temperatures, and consequently to lower flame front velocities [29].

2.2. Apparatus

The syngas produced during the biomass gasification process is burned into a Honda ICE, designed to work with gasoline and adapted to operate with syngas [13]. The gasifying agent used is a quantity of air, between 20 and 40% of the theoretically value necessary for a complete combustion. Only the biomass feed system and the reactor are necessary for gasifying the biomass while the syngas needs to be treated in a cleaning system due to the amount of solids and tars contained therein.

The experimental gasification plant is composed of the following components: the reactor (Fig. 1), the gas cleaning system (Fig. 2) and the water treatment system (Fig. 3).

2.2.1. The reactor

Different endothermic and exothermic reactions take place in the reactor (Fig. 1), while the biomass is converted into a lower heating value gas, syngas [11]. Four different zones can be distinguished: drying, pyrolysis, oxidation and reduction, where the different chemical reactions are produced. The combustion or oxidation zone has the highest temperature due to the exothermic nature of the reactions (800–900 °C). Two meter devices are incorporated in this area: a K-type thermocouple is settled in the area near the air inlet pipe and another one just 1 cm below the throat. The reduction zone is a truncated cone where endothermic reactions among CO_2 and H_2O with CO and H_2 are carried out. At the end of the reduction zone, a grid (number 5) is located to prevent undesirable biomass loss. The reactor is equipped with a biomass deposit (number 6) of a volumetric storage capacity equal to 226 l, equivalent to 45 kg of pellets with a bulk density of 400 kg/m^3. After filling the deposit with biomass and closing the upper valve (number 1), the lower valve (number 2) should be open in order to enable the biomass to enter the reactor. In this way, the control of the air entering the reactor is possible and the system is preserved from working under vacuum. The air speed is settled around 30–35 m/s to guarantee that the combustion temperature arises from 550 to 1000 °C at the top of the throat so as tars concentration in the syngas will be significantly lower. In order to reduce the holes formation, a bed-bridge breaker lever (number 3) and an electrical vibrator (number 4) have been installed (Fig. 1). The holes are pockets of air that made reactions following

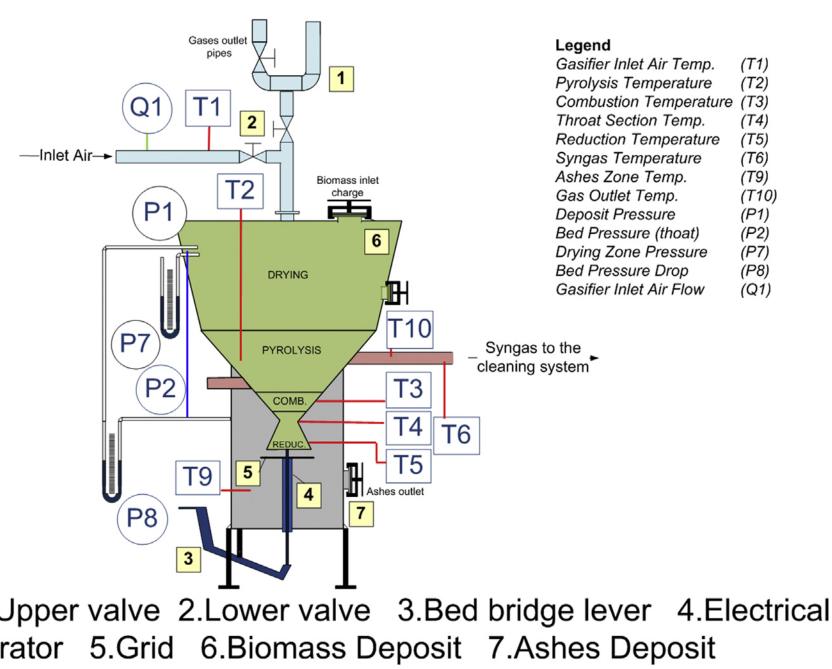

Fig. 1. The gasifier scheme.

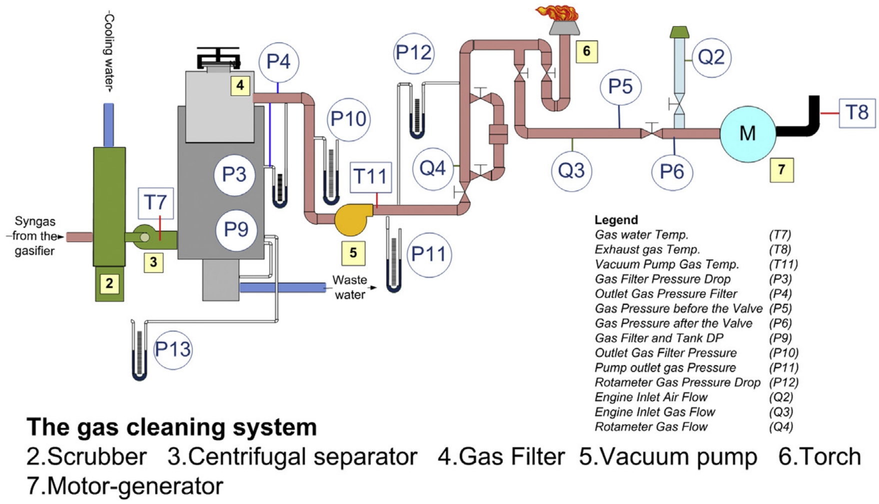

Fig. 2. The gas cleaning system.

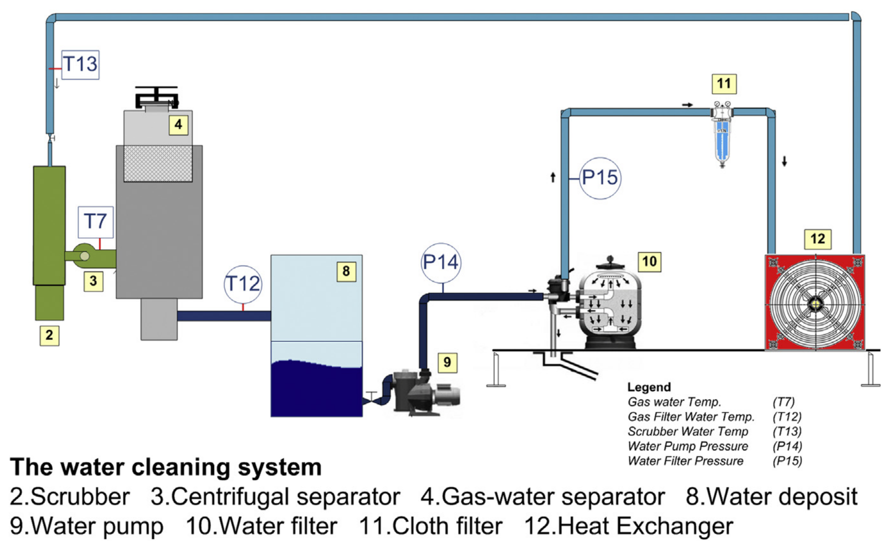

Fig. 3. The water treatment system.

preferential directions lowering the efficiency. They are frequent into the combustion, pyrolysis zones and influenced by the biomass moisture and size [9]. Indeed the bed-bridge breaker lever and the electrical vibrator allow evacuating the char that should clog the throat and the flow of larger pellets (1.5 × 1.5 × 1.5 cm). In this way, these components ensure that an adequate new amount of biomass is always present into the reaction zone and takes part into the gasification process, improving the efficiency. At the same time, they are able to reduce the bed pressure drop and keep it under a proper value. Finally, there is an ashes deposit (number 7) where charcoal and ashes that have not been gasified are stored and evacuated.

2.2.2. The gas cleaning system

The gas cleaning system removes the ashes and charcoal residues still present into the produced gas (Fig. 2). The syngas leaving the gasifier needs to be cleaned to have high process efficiency and avoid damages of the ICE. This system is composed of the following elements: scrubber (number 2), centrifugal separator (number 3), gas filter (number 4) and centrifugal vacuum pump (number 5). The scrubber refrigerates and separates residue solids from the syngas. It determines the condensation of tars present in the syngas. The centrifugal separator eliminates the water, tar and solids contained into the syngas. The gas filter separates particles and tars which could not be removed by the centrifugal separator and forces it to pass sequentially through a bed of stones, bubbling bells and a bed of chips in order to be dried. Then the syngas flows through a nylon filter of 200 microns, which retains solid particles and chips, and finally through the cotton filter where the residual moisture eventually still present is eliminated. At the end, the syngas leaves the filter and is sent to the ICE. As the centrifugal separator, the vacuum pump creates the required depression to allow the air to enter the gasifier, react with the biomass and produce the syngas. The gasifier is designed to work under depression, so that the gas circuit must be sealed to prevent any air infiltration. The torch (number 6) is used to burn the excess of syngas not used for producing electricity. The ICE (number 7) adopted is a Twin Commercial Honda Engine 630 cc working with gasoline [30]. This engine is adapted to operate with syngas with a consequently reduction in the power production compared to its operation with gasoline (about a 28%) [11].

2.2.3. The water treatment system

The water system (Fig. 3) has the function of removing solids and tar from the water used into the gas system for refrigerating and cleaning the syngas. Thus, water can be reused and the syngas can be continuously cleaned, reducing the cost and the amount of the waste water. This circuit is composed of the following elements: water deposit (number 8), water pump (number 9), water filter (number 10), cloth filter (number 11) and heat exchanger (number 12).

In the water circuit, there are two water tanks. The water deposit has a capacity of 100 l. It collects by gravity the water which comes out from the gas filter. Once the water leaves the deposit, it is sent to a second tank, the water filter (500 l), by means of a centrifugal pump.

The water filter eliminates the solids and tars suspended in the water. The cloth filter has a pore size of 60 microns and prevents the particles of sand and chips to reach the heat exchanger. The heat exchanger reduces the water temperature so it can be continuously used for the syngas cooling. Figs. 1–3 show schematically the location of the measurement points and devices in the gasification plant.

3. Considerations on the bed pressure drop and the throat sizing

Experimental tests were performed according to two different reactor configurations. To ensure the data reproducibility the gasification plant has been fueled with a pellets source characterized by the same chemical and geometrical properties (i.e. diameter, moisture, composition, etc.) during each tests.

3.1. Analysis of the response parameter: bed pressure drop

Previous studies have shown how some ranges of the response parameter (bed pressure drop) do not guarantee the reliable operation of a fixed bed gasifier [31–33]. The pressure drop should properly range between 2.5 and 10 mbar with an optimum value around 6.3 mbar. Instead, pressures into range lower than 2.5 mbar are typical values achieved in the following samples:

- The insufficient amount of biomass into the gasifier deposit.
- The lack of homogeneity in the gasification process. Gasification reactions take place only in specific area into the reactor.

On the other hand, pressure drop values greater than 12 mbar determine:

- The mismatch of the air-fuel ratio in the ICE with a consequent decrement of the cumulative efficiency.
- The decrement of the volumetric efficiency where the volumetric efficiency is the ratio between the real volume and the maximum volume of the gasifier. Generally this value falls within a range between 0.7 and 0.9.
- The instability of the bed pressure drop, which suddenly increases and decreases during the operation of the gasifier.

In order to contain the research costs, a previous theoretical analysis has been carried out on the gasifier design to predict the influence of the throat diameter on the response parameter, pressure drop, before operating the technical modification. The trend of the bed pressure drop with a different throat diameter has been theoretically evaluated. Throat diameters larger than 10 cm have been demonstrated to negatively affect the cumulative efficiency of the gasification process [34]. So a throat diameter ϕ_2 equal to 10 cm has been chosen and its influence on the bed pressure drop has been investigated.

Into the fixed bed gasifier, the transfer of heat and mass takes place between the fluid and solid phases and the transfer has been supposed to be steady state. The fixed bed geometry itself has been considered cylindrical and the flow of the fluid through the bed parallel to the axis of the cylinder. Radial flow of the fluid has not been taken into account.

The major design parameters are the pressure drop across the fixed bed, and the heat and mass transfer coefficients between the fluid and the surface of the solid phase. Diffusion of heat and mass into the interior of the solid phase can be a significant mechanism of transfer, but it is common to employ lumped transfer coefficients at the surface to account for the internal diffusion, and to use average solid temperatures and concentrations in the design calculations.

According to the principle of the mass conservation, the continuity equation for the throat section of the ϕ_2 diameter is expressed in cylindrical coordinates (r = radius; Θ = angle) by (1):

$$\dot{m}_{a,in} \approx \dot{m}_{g,out} \rightarrow (\rho_a A_0 v_0)_{in} \approx (\rho_g A_2 v_2)_{out} \quad (1)$$

$$\left(\frac{\partial \rho_a}{\partial t} r_0 dr d\theta dz\right)_{in} \approx \left(\frac{\partial \rho_g}{\partial t} r_2 dr d\theta dz\right)_{out}$$

Alike, according to the first law of the thermodynamics applied to a steady-flow system where net frictional forces are negligible, the energy balance should be applied and written between the two points of the bed reactor, air inlet section and outlet gas section, as follows:

$$\left(\frac{P_0}{\rho_a} + \frac{v_0^2}{2} + g z_0\right)_{in} \approx \left(\frac{P_2}{\rho_g} + \frac{v_2^2}{2} + g z_2\right)_{out} \quad (2)$$

Pressure drop across a fixed bed has been calculated from the empirical formula proposed by Ergun in 1952 [35]:

$$\frac{\Delta P_2}{L} \approx \left(\frac{c_1 \rho_m \cdot u^2 (1-\varepsilon)}{d \cdot \varepsilon^3}\right) + \left(\frac{c_2 \cdot \gamma \cdot u \cdot (1-\varepsilon)^2}{d^2 \cdot \varepsilon^3}\right) \quad (3)$$

where ΔP is the pressure drop, L is the length of the reduction zone, d is the equivalent diameter of the particle, defined as the equivalent volume sphere (=6 × volume/surface area), ε is the porosity (porosity = free volume/total volume), u is the superficial velocity based on flow through an empty fixed bed, Υ is the fluid viscosity and c_1 and c_2 are correlation values obtained by regression of experimental data. The values of c_1 and c_2 for randomly packed spherical particles have been adopted ($c_1 = 1.8$ and $c_2 = 180$). The continuity balance represented by (1) on the bed of the reactor shows that for a constant air inlet flow of 15 m^3/h, the gas flow speed for the ϕ_2 diameter is about 0.531 m^2/s (Table 3). As expected, the increase in the throat diameter causes a decrease in the outlet flow velocity, but the choice of a ϕ_2 diameter equal to 10 cm determines an outlet gas speed value equal to a half of the experimental gas flow speed measured for the diameter ϕ_1 equal to 7 cm and for the same constant inlet air flow of 15 m^3/h (Table 3).

The thermodynamic balance and the Ergun formula expressed by (2) and (3) give the possibility to evaluate the behavior of the bed pressure drop for ϕ_2 diameter. The obtained data shows that the pressure drop is lower than in case of a throat diameter ϕ_1 ad for a constant air inlet flow. The pressure drop decreases when the throat section increases for a fixed inlet air flow but the main result is that the obtained pressure drop is properly set into the recommended range as specified before (Fig. 5). The theoretical analysis for the throat diameter of 10 cm underlines the positive effect that the modification could determine on the bed pressure drop and supports the throat technical implementation. Fig. 5 shows the theoretical pressure drop profile as a function of the air inlet flow parameter related to the diameter ϕ_2. The electrical power has been estimated and calculated considering a constant LHV of 1200 kcal/m^3. This value is the average value of the experimental LHV monitored and acquired during the operation of the experimental plan at the first campaign.

3.2. Description of the throat modification

Measurements carried out during tests allow to monitor the response parameter, bed pressure drop and the operating parameters, syngas production, air inlet flow, etc. in order to assess the influence of the throat sizing on them. The reactor configuration for the first campaign is characterized by a throat diameter equal to 7 cm, with a corresponding throat section of 0.0038 m^2. The biomass flow measured is about a 10 kg/h with a syngas production of about 21 Nm^3/h. Therefore, the biomass processing capacity is 2.67 kg/h cm^2 (0.55 m^3/h m^2) and the gas design speed in the throat is calculated about 1.56 m/s. The actual speed is determined to be greater than the design speed due to the reduction of the gas passage area caused by the char and by the use of a perforated plate. During the second campaign, the modification realized on the gasification plant consists into the increment of the throat diameter from 7 cm to 10 cm with a corresponding increase in throat section of 0.0078 m^2 (about 50%). The cross sectional area of the throat is a same circular opening geometry during both campaigns.

As shown in previous, studies the throat angle influences the cumulative conversion efficiency along the reduction zone axis. Smaller throat angles increase the cumulative efficiency if also a longer reduction zone is adopted [36,34]. In this application, a throat angle of 61° is used for the first campaign and an angle of 58° for the second one with a length of the reduction zone (L) respectively of 8 cm and 12 cm. The gasifier had 6 nozzles with 10 mm diameter for the injection of air.

4. Test methodology and experimental procedure

The test methodology adopted for this research consists of the following steps (Fig. 4):

1. Preparation of the pellets.
2. Turning on the gasification plant.

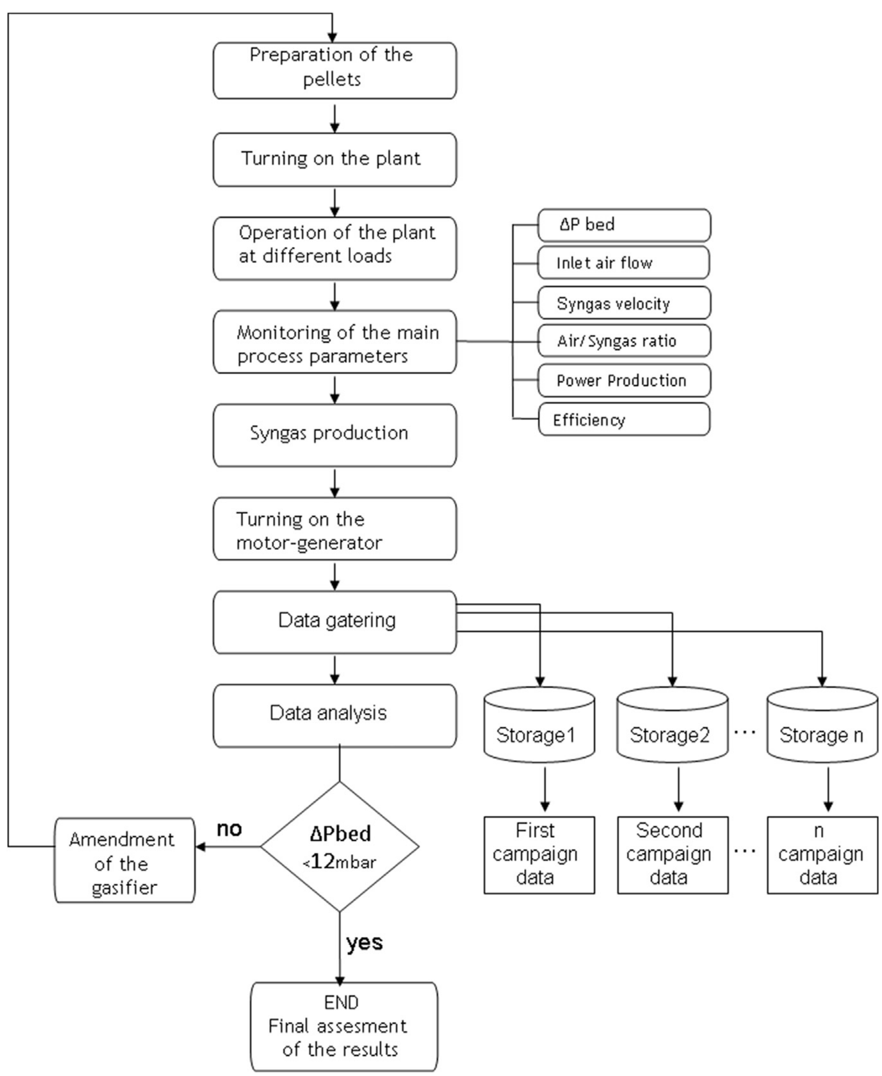

Fig. 4. Test methodology.

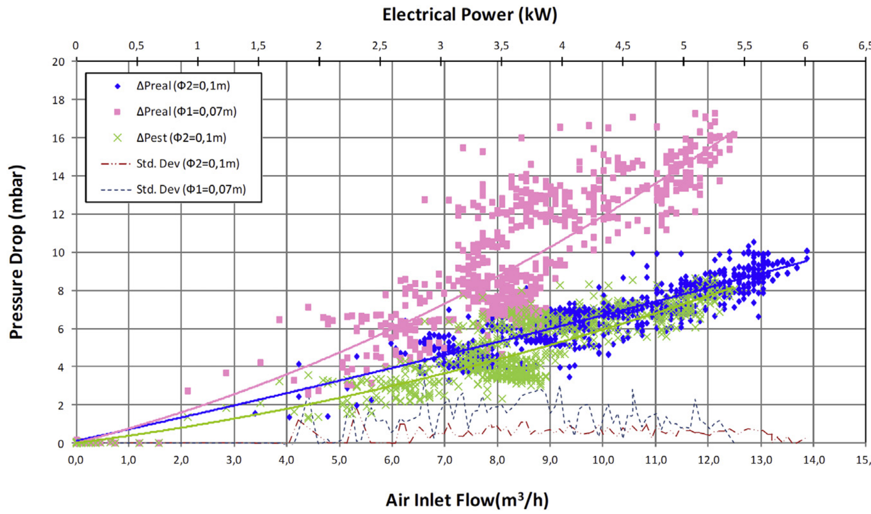

Fig. 5. Bed pressure drop as function of inlet air flow.

3. Operating the plant at different loads, increasing the load from 8 to 15 m^3/h.
4. Turning on the motor–generator.
5. Monitoring of the response parameter: Fixed bed pressure drop [bar].

Pressure drop value should be lower than 12 mbar as it will be discussed in the following paragraph.

6. Data acquisition for the first campaign with the experimental parameter 'throat diameter' equal to 7 cm and monitoring of the operating parameters of the gasification plant listed below:
   - Air-fuel ratio
   - Inlet air flow [Nm^3/h]
   - Syngas flow produced [Nm^3/h]
   - Syngas velocity at the throat section [m/s]
   - Electrical power produced [kW_e]
   - Efficiency
7. After the first campaign, a modification of the reactor design is realized. The throat diameter is incremented from 7 to 10 cm.
8. Repeat the same procedure for the assessment of the influence of the experimental parameter on the driving process variables and on the system operation.
9. Data acquisition for the second campaign and monitoring of the same operating parameters listed before.
10. Evaluation of the results obtained through a comparison between the two different configurations.

During the two campaigns, the response variables listed before (syngas production, electrical power, etc.) have been monitored by the acquisition and measurement system. A detailed analysis on the influence of the reactor throat size on the process parameters has been carried out. Tests carried out on the different reactor configurations have been divided into two campaigns and for each tests the input parameters are shown in Table 2.

5. Experimental results and discussions

The results hereby presented were obtained in two campaigns. The following transitory state effects associated to gasifier operation have been properly considered and addressed, including:

- The ignition of the gasifier
- The ignition of the internal combustion engine
- The disconnection of the power plant due to the pressure drop instability effect
- The operation by electrical vibrator
- The operation by breaking bed handle

Table 2
Test input parameters.

		Test duration		Biomass (kg)		Air flow (m^3/h)		Biomass flow	Air/biomass	Air/stoich.
First campaign	1 TEST 03/13	Start	12.53	Initial	34.95	Average	8	6.12 kg/h	1.3 m^3/kg	28.30%
		End	13.42	Final	29.95	Min	7			
		Time	49 min	Consump.	5	Max	9			
	2 TEST 03/21	Start	12.18	Initial	35.55	Average	8.6	6.68 kg/h	1.82 m^3/kg	39.82%
		End	14.09	Final	28	Min	4			
		Time	66 min	Consump.	7.5	Max	12.5			
	3 TEST 03/15	Start	13.01	Initial	42.1	Average	8.89	22.73 kg/h	0.39 m^3/kg	8.40%
		End	14.07	Final	31.95	Min	8			
		Time	111 min	Consump.	10.05	Max	12			
Second campaign	4 TEST 04/13	Start	11.10	Initial	42.8	Average	11.17	7.58 kg/h	1.48 m^3/kg	31.80%
		End	13.15	Final	23.85	Min	8			
		Time	150 min	Consump.	18.9	Max	16.07			
	5 TEST 04/18	Start	11.14	Initial	44.45	Average	10,5	6.05 kg/h	1.74 m^3/kg	37.30%
		End	13.54	Final	32.65	Min	8			
		Time	117 min	Consump.	11.8	Max	15.06			

Table 3
Gas flow velocity at the constant air inlet flow for different throat diameters.

Air inlet flow	$\dot{Q}_a = constant$	
(m^3/h)	15	
Throat diameter	Φ_1	Φ_2
(m)	0.07	0.1
Throat section	*A1*	*A2*
(m^2)	0.0038	0.0078
Gas flow speed	V_1	V_2
(m^2/s)	1.08	0.531

- Accidents happened during the tests (breakage of a thermocouple, increase in the level of water in the filter, etc.)

In the following results, some of the most significant parameters are presented in order to highlight the consequences of increasing the throat diameter from a value of 7 cm to a value of 10 cm. The first campaign was performed before the modification of the throat; the second one was carried out when the change had been already made. The fuel used for the tests was pellets in all of the cases characterized by the constant chemical and geometrical properties (i.e. diameter, moisture, composition, etc.). According to the results obtained from the different tests, it is possible to determine the way in that the diameter of the throat influences the principal response parameter, bed pressure drop and consequently the inlet air flow, the electrical power production, and the syngas production.

5.1. Bed pressure drop and inlet air flow: experimental data achieved

Fig. 5 shows the experimental data achieved during the two campaigns. The trend of the pressure drop as a function of the inlet air flow is represented for the throat diameter of 7 cm and 10 cm. The pressure curves presented in (4) and (5) are not generalized but specific formulas valid for the experimental gasifier improved in this work.

The profile of both curves shows that, when the inlet air flow increases, the pressure drop increases quadratically.

$$\Delta P_1(\varphi_1 = 0{,}07) = 4.8\cdot10^{-2}\cdot\dot{Q}_a^2 + 7.05\cdot10^{-1}\cdot\dot{Q}_a + 6\cdot10^{-3} \qquad (4)$$

$$\Delta P_2(\varphi_2 = 0{,}10) = 3.9\cdot10^{-3}\cdot\dot{Q}_a^{\;2} + 6.23\cdot10^{-1}\cdot\dot{Q}_a + 6.73\cdot10^{-2} \qquad (5)$$

The quick increment of the bed pressure drop for the throated reactor of 7 cm limits the maximum air inlet flow available to 7 m^3/h. The variation of the bed pressure drop values is out of the acceptable pressure range for the proper operation as discussed before.

The pressure curve represented by (5) for the throat diameter of 10 cm is the experimental curve resulted from the second campaign of experimental tests after the performance of the throat modification. The throat modification supported by the previous theoretical study positively affects the trend of the pressure-air inlet flow curve for the diameter of 10 cm (Fig. 5). This experimental curve for the diameter ϕ_2 shows the proper variation of the pressure drop data between 2.5 and 10 mbar as required for the correct operation of the gasification plant and already suggested by the estimated curve. Actually, for values of inlet air flow below 11 Nm^3/h, the experimental pressure drop differs from the theoretical value by about 1.5 mbar, while the difference between the two values is reduced to 0.5 mbar when the air flow is greater than 11 Nm^3/h (Fig. 5).

Table 4 shows the trend of the inlet air flow in correspondence to the maximum values of pressure drop. Complementarily, it also shows the trend of the bed pressure drop in correspondence to the maximum values of the inlet air flow.

According to the experimental data obtained during the tests, the following specific conclusions can be obtained:

- During the third test with a throat of 0.07 m, the maximum inlet air flow reached is 12.3 Nm^3/h while during the fifth test, with throat of diameter of 0.1 m, it is 16.1 Nm^3/h. The increment is about 31.6%.
- The maximum pressure drop is equal to 17.2 mbar for the diameter ϕ_1, while it is equal to 14.5 mbar for the diameter ϕ_2. The maximum pressure drop decreases by 15.7%
- At the same pressure drop of 9.8 mbar, the maximum air flow is equal to 11.8 Nm^3/h for the throat diameter of ϕ_1. For the throat diameter of ϕ_2, the maximum air flow is equal to 16.7 Nm^3/h. Increasing the throat diameter, the maximum air flow increases at the same pressure drop.

It means that, for the same value of maximum pressure drop, a larger diameter of the throat of the gasifier increases the inlet air flow.

The modification had also influenced the gasification process stability. Actually the following results can be achieved:

- For a throat diameter ϕ_1, the variation of the pressure drop is highly unstable when the air flow varies. In fact, a variation of pressure drop of 8.7 mbar corresponds to the variation of inlet air flow of 2.85 Nm^3/h. Its maximum value is equal to 15.9 Nm^3/h. This value is out of the pressure range for a proper operation of the gasifier.
- For the throat diameter ϕ_2, the variation of the pressure drop is smaller and stable when the air flow varies. In fact, a variation of pressure drop of 0.3 mbar corresponds to the variation of inlet air flow of 1 m^3/h. Its maximum value is equal to 9.8 Nm^3/h. This value falls into the range of operating pressure of the gasifier.

Table 4
Influence of the throat diameter on the driving parameter: maximum values.

Throat diameter		First campaign			Second campaign	
		$\Phi_1 = 0.07$ m			$\Phi_2 = 0.1$ m	
Parameter		Test 1	Test 2	Test 3	Test 4	Test 5
$\dot{Q}_a$ max	m^3/h	9.5	11.8	12.3	15.1	16.1
$\Delta P\_\dot{Q}_a$ max	mbar	7.2	9.8	15.9	9.5	9.8
ΔP max	mbar	11.9	13.8	17.2	10.7	13.6
$\dot{Q}_a\_\Delta P$ max	m^3/h	7.9	10.3	12.1	8.5	14.5
Q_g max	m^3/h	15.8	19.7	20.5	25.1	26.8

In Table 5, the pressure drop values are processed according to the set point of inlet air flow. The set point has to maintain a constant flow of inlet air and it is set from the outside. When the value of the inlet air flow differs from the set point, the system modifies the frequency of the fan and it brings the incoming air flow back to the initial fixed value. The set point of inlet air flow is a significant parameter for the gasifier. The set point is zero during the ignition of the internal combustion engine. Actually, during this phase, this parameter becomes meaningless because the volumetric flow rate of inlet air varies, depending on the needs of the engine (in other words, as a function of the air-fuel ratio of the engine).

Table 5
Pressure drop according to the set point of inlet air flow.

First campaign						Second campaign					
Diameter of throat $\Phi_1 = 0.07$ m						Diameter of throat $\Phi_2 = 0.1$ m					
03/21	Test 2		03/15	Test 3		04/18	Test 4		04/13	Test 5	
Set	Q_{air}	ΔP	Set	Q_{air}	ΔP	Set	Q_{air}	ΔP	Set	Q_{air}	ΔP
0	0.1	2.5	6	6.9	8.6	0	5.5	3.6	0	5.94	3.8
5	5	5.7	8	8	8.7	8	8.4	5.7	10	9.79	3.6
8	8.4	11.7	9	8.7	12.7	9	8.8	3.6	11	11.19	7.5
9	8.8	8.9	10	9.7	12.4	9	8.8	5.7	11	11.43	7.2
9	6.5	5.4	11	10.7	14.3	10	9.5	5.4	12	11.69	7.7
10	9.8	11.8	12	11.5	14.1	10	10.3	7.4	13	12.34	8.2
11	11	12	13	12.1	16.3	11	10.8	7.4	14	13.75	10.1

From the analysis of the inlet flow air as a function of pressure drop, the next conclusions can be stated:

- For the throat diameter ϕ_1, in the range of volumetric flow rate between 6 and 12 Nm^3/h, the pressure drop varies between 5.4 and 12.6 mbar while for the throat diameter ϕ_2 it is just between 4 and 8.2 mbar
- For ΔQ a equal to 4 Nm^3/h, the pressure drop is 7.2 mbar for ϕ_1, while it takes the value of 4.2 mbar for ϕ_2

The pressure drop varies significantly for diameter ϕ_1 when the inlet air flow varies, while the difference is much less significant for diameter ϕ_2. The pressure drop variability depends on the throat diameter in a way that it will be as greater as smaller the throat diameter is.

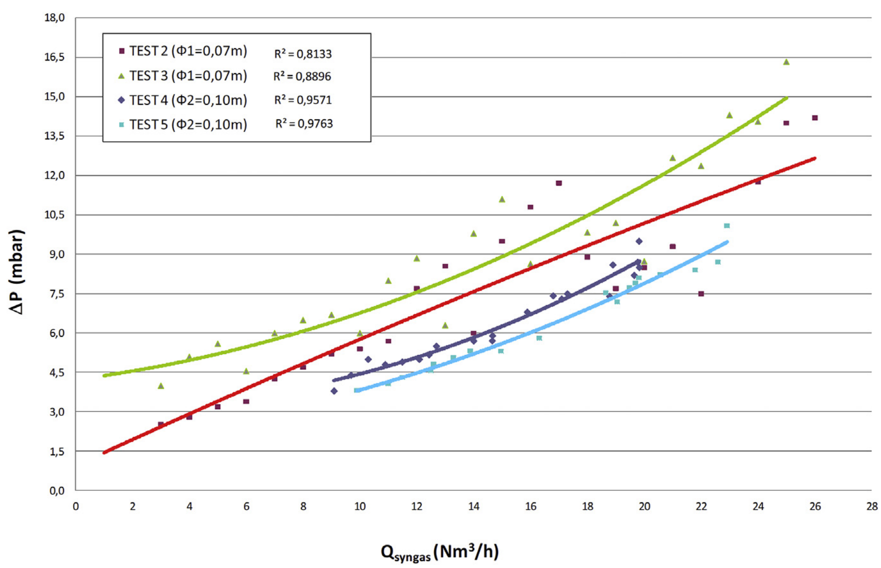

Fig. 6. Syngas production as function of bed pressure drop.

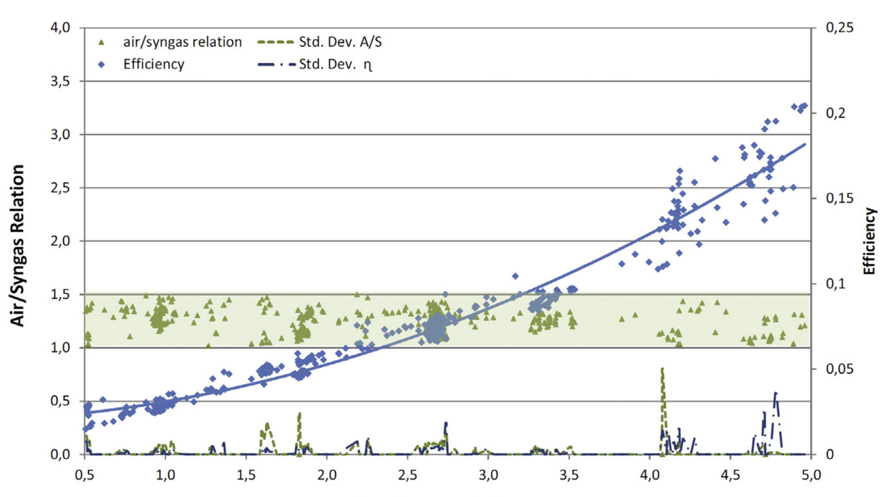

Fig. 7. Electrical power production and the air syngas rate trend.

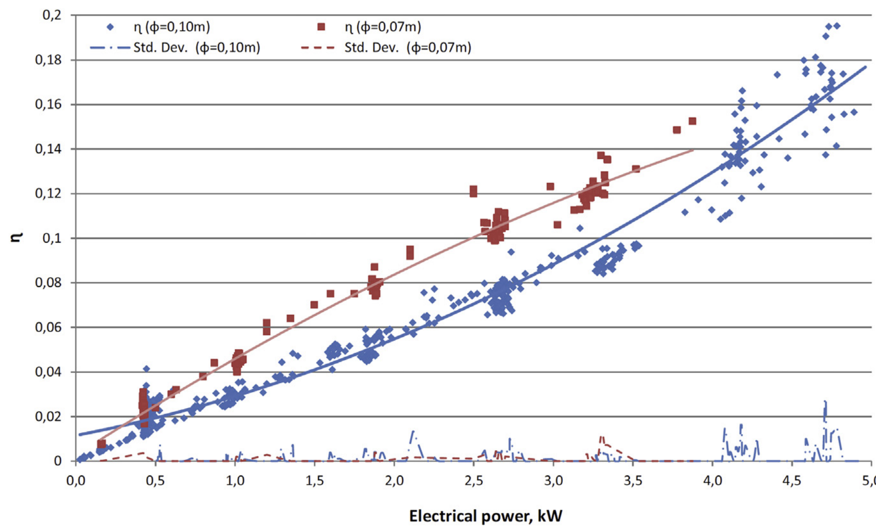

Fig. 8. Efficiency as function of the electrical power production.

5.2. Syngas production

Table 4 highlights the maximum value of the syngas produced during the plant operation after the realization of the modification on the reactor. The results show that:

- The maximum volumetric flow rate of syngas increases when the diameter of the throat increases. It grows from 20.5 Nm^3/h to 26.8 Nm^3/h.
- The increment of syngas obtained is about 30.7%.

Fig. 6 shows the syngas production of the gasifier during each test as function of the pressure drop. For the same value of maximum pressure drop, a larger diameter of the throat of the gasifier increases the inlet air flow and consequently, the syngas flow also increases.

5.3. Electrical power production and air syngas rate

Fig. 7 shows the pressure drop as a function of the electrical power supplied by the power plant for the two different configurations. Regarding the values of electrical power, they were measured by means of a network analyser. For the first configuration, the pressure drop trend affects the syngas production and consequently limits the power production. Actually due to the instability of the bed pressure drop for the throat diameter of 7 cm, the maximum power production achieved is only about 3 kWe (Fig. 8). Instead, the throat modification positively affects the operation of the gasifier by the increment of the electrical power production in about 40%. The maximum electrical power achieved for the inlet air flow of 11.2 Nm^3/h is 5 kWe. Fig. 7 shows the performance of the air-syngas ratio according to the power production and the efficiency. It can be observed that the system works properly as this ratio varies between 1 and 1.5, which is the range of excellent work for the air-fuel ratio of a gasification plant [13]. The equation that describes the trend is (6):

$$A/S = -1.86 \cdot 10^{-2} \cdot P_{elec} + 1.24 \qquad (6)$$

where A/S is the air-syngas rate and P_{elec} is the electrical power at the generator terminals. It can be seen that the electrical power tends to zero when the value A/S is 1.24. The range considers only the case of a loaded engine.

5.4. Efficiency

Following, the trend of the efficiency of the system motor-generator as a function of the electrical power of the gasification plant is analyzed (Fig. 8). The increment of about 50% of the throat section determines that the efficiency also increases, reaching the maximum value of 0.21 at the maximum value of electrical power 5 kWe. While during the first campaign the maximum value reached for the motor engine efficiency is just 0.14, an increment of about 35% is achieved by the assessment of the throat modification.

6. Conclusions

This paper evidences as performing the proposed design modification on the throat of a downdraft gasifier, a significant improvement on the reliability can be achieved. The increment of the throat diameter from 7 to 10 cm, corresponding to an increment of about 50% of the throat section, reduces the bed pressure drop up to the 16% and sets its variation into a favorable range of management. The greater stability reached by the pressure drop during the power plant operation ensures the continuous schedule of the gasification plant, reducing the disturbance of safety control system (electrical vibrator, break bed system, etc.). An increment of the air inlet flow between 10 and 16 Nm^3/h is achieved, which increases the syngas production in about 31% (from 11.8 Nm^3/h to 16.7 Nm^3/h) compared to the original plant configuration. The experimental results demonstrate an increment of the electrical power produced by the gasification plant of about 40% (from 3 kWe to 5 kWe) and a correspondent increment of the motor generator efficiency up to 35% (from 0.14 to 0.21) with an adequate air-syngas ratio varying properly between 1 and 1.5. As it has been demonstrated, the throat diameter of a downdraft gasifier is a very sensitive parameter which strongly affects the production of syngas and, consequently, the efficiency of the whole plant. Readers have in this paper a practical case where this issue has been addressed, performing the required modifications in a real gasifier with the abovementioned positive results.

References

[1] IEA. World Energy Outlook: Executive Summary 2000. Available online at: www.worldenergyoutlook.org.
[2] Kai Z, Jian C, Yanjun G, Honggang C, Yongping Y, Jianchun J. Lignocellulosic biomass gasification technology in China. Renew Energy 2013;43:175–84.
[3] Kang Q, Appels L, Tan T, Dewil R. Bioethanol from lignocellulosic biomass: current findings determine research priorities. Sci World J 2014;13.
[4] Budzianowski WM. Modelling of CO_2 content in the atmosphere until 2300: influence of energy intensity of gross domestic product and carbon intensity of energy. Int J Glob Warm 2012;4:35–7.
[5] Jiang-Jiang W, Zi-Long X, Hong-Guang J, Guo-hua S, Chao F, Kun Y. Design optimization and analysis of a biomass gasification based BCHP system: a case study in Harbin, China. Renew Energy 2014;71:572–83.
[6] McKendry P. Energy production from biomass (part 1): overview of biomass. Bioresour Technol 2002;83:37–46.
[7] Montuori L. Integration of renewable energy sources in microgrids coordinated with demand response resources: application to a biomass gasification plant coupled with an internal combustion engine for power generation. Dissertation Project. Spain: Universidad Politécnica de Valencia; 2013.
[8] Basu P. Biomass gasification and pyrolysis: practical design and theory, vol. 2. Elsevier Inc.; 2010. p. 83–102.
[9] Rajvanshi AK. Alternative energy in agriculturevol. 2. NARI; 2014. p. 83–102.
[10] Perlack RD, Stokes BJ. U.S. billion-ton update: biomass supply for a bioenergy and bioproducts industry. US Department of Energy; 2011.
[11] Sims REH. Bioenergy to mitigate for climate change and meet the needs of society, the economy and the environment. Mitig Adapt Strat Glob Change 2003;8:349–70.
[12] Industry statistics: annual world ethanol production by country. Renewable Fuels Association c2005–c2015.
[13] Sharma AK. Experimental study on 75 kWth downdraft (biomass) gasifier system. Renew Energy 2009;341:1726–33.
[14] Graciosa Pereira E, Nogueira da Silva J, de Oliveira JL, Machado CS. Sustainable energy: a review of gasification technologies. Renew Sustain Energy Rev 2012;16:4753–62.
[15] Peres GAP, Lunellia B, FIlhoa R. Application of biomass to hydrogen and syngas production. Chem Eng Trans 2013;32:2013.
[16] Smoliński A, Howaniec N, Stańczyk K. A comparative experimental study of biomass, lignite and hard coal steam gasification. Renew Energy 2011;36:1836–42.
[17] Montuori L. Experimental evaluation of a biomass gasification plant coupled with an internal combustion engine for power generation. Economic viability analysis by Homer Energy Simulator. Master Degree Thesis. Italy: Università degli Studi di Napoli Federico II; 2013.
[18] Montuori L, Alcazar-Ortega M, Alvarez-Bel C, Domijian A. Integration of renewable energy in microgrids coordinated with demand response resources: economic evaluation of a biomass gasification plant by Homer Simulator. Appl Energy 2014;132:15–22.
[19] Zhang L, Xu C, Champagne P. Overview of recent advances in thermochemical conversion of biomass. Energy Convers Manag 2010;51:969–82.
[20] Kirubakaran V, Sivaramakrishnan V, Nalini R, Sekar T, Premalatha M, Subramanian P. A review on gasification of biomass. Renew Sustain Energy Rev 2009;13:179–86.
[21] Martínez JD, Mahkamov K, Andrade R, Electo E. Syngas production in downdraft biomass gasifiers and its application using internal combustion engines. Renew Energy 2009;38:1–9.
[22] Bellomare F, Rokni M. Integration of a municipal solid waste gasification plant with solid oxide fuel cell and gas turbine. Renew Energy 2013;55:490–500.
[23] Asadullah M. Barriers of commercial power generation using biomass gasification gas: a review. Renew Sustain Energy Rev 2014;29:201–15.
[24] Sang Jun Y, Yung-Il S, Yong-Ku K, Jae-Goo L. Gasification and power generation characteristics of rice husk and rice husk pellet using a downdraft fixed-bed gasifier. Renew Energy 2012;42:163–7.
[25] Sheth PN, Babu BV. Experimental studies on producer gas generation from wood waste in a downdraft biomass gasifier. Bioresour Technol 2009;100:3127–33.
[26] Tinaut FV, Melgar A, Pérez JF, Horrillo A. Effect of biomass particle size and air superficial velocity on the gasification process in a downdraft fixed bed gasifier. An experimental and modelling study. Fuel Process Technol 2008;89:1076–89.
[27] Guangul F, Sulaiman S, Ramli A. Study of the effects of operating factors on the resulting producer gas of oil palm fronds gasification with a single throat downdraft gasifier. Renew Energy 2014;72:271–83.
[28] Gunarathne D, Jatunarachchi S, Senanayake NS. The effect of throat diameter on the performance a downdraft biomass gasifier. Int J Energy Eng 2013:171–5.
[29] Bhavanam A, Sastry RC. Biomass gasification processes in downdraft fixed bed reactors: a review. Int J Chem Eng Appl 2011;2:6.
[30] Commercial catalogue of Honda engines. Available online at: http://engines.honda.com; June, 2012.
[31] Gunarathne S, Chmielewski JK, Yang W. Experimental plant pressure drop prediction of a gasifier bed with cylindrical biomass pellets. Appl Energy 2014;113:258–66.
[32] Sadaka S. Gasification. Center for Sustainable Environmental Technology; 2004. Nev U.S.
[33] Azzone E, Morini M, Pinelli M. Development of an equilibrium model for the simulation of thermochemical gasification and application to agricultural residues. Renew Energy 2012;46:248–54.
[34] Kumar SS, Pitchand K, Natarajan E. Modeling and simulation of downdraft wood gasifier. J Appl Sci 2008;8:271–9.
[35] Carpinlioglu MO, Ozahi E. A simplified correlation for fixed bed pressure drop. Powder Technol 2008;187:94–101.
[36] Ojolo SJ, Orisaleye JI. Design and development of a laboratory scale biomass gasifier. J Energy Power Eng 2010;4:16–23.